Radio Science, Volume 35, Number 1, Pages 133–140, January–February 2000

Calibration of zenith hydrostatic delay model for local GPS applications

Y. Liu, H. Baki Iz[1], and Y. Chen

Department of Land Surveying and Geo-Informatics, The Hong Kong Polytechnic University, Hung Hom, Kowloon, Hong Kong

Abstract. Determination of dry zenith delay, DZD, is important for separating wet zenith delay with high accuracy from Global Positioning System (GPS) measurements. The existing models are usually for the calculation of the zenith hydrostatic delay, ZHD. Because the zenith hydrostatic delay includes the contribution of water vapor and is also not accurate enough, the DZD, approximately replaced by ZHD, will induce ~2 cm error into local GPS applications. In this study we calibrate a popular ZHD model, namely, the Saastamoinen model for local GPS meteorology, using radiosonde data. We test the calibrated model by comparing the predicted delays from the calibrated model against the observed delays from radiosonde data that are not included in the calibration solution. The calibrated model shows 20 mm improvement over the uncalibrated model predictions over the same period. A comparison of the DZDs calculated from GPS measurements over a month period with calibrated and uncalibrated ZHD model predictions shows 15 mm average improvement.

1. Introduction

The tropospheric delay is an important error source in space geodetic observations. The conventional approach is to eliminate or reduce its influence via empirical models or to estimate its influence through unknown parameters. A by-product of this latter approach is the spatial and temporal resolution of the tropospheric zenith delay, which is beneficial for weather research and global climate monitoring.

In the case of Global Positioning System, GPS, the signal is affected by the tropospheric delay when it crosses the troposphere from GPS satellite to ground receiving station. This delay can be broken into two components: the wet delay, which is caused by the wet atmosphere or water vapor, and the dry delay, which is caused by the dry atmosphere. One of the basic objectives of GPS meteorology is to acquire the spatial and temporal precipitable water vapor content derived from the wet zenith delay from the GPS measurements. Hence, separating the wet zenith delay from the tropospheric zenith delay, which is the sum of the wet zenith delay and the dry zenith delay, DZD, is needed for accurate GPS meteorological applications. Although DZD can be accurately computed from radiosonde data, this is a very costly approach to implement. Instead, empirical models that depend on less costly surface meteorological data are developed for this purpose.

DZD depends on the shape of the profile with height and the dry air/water vapor mix ratio. However, there is no specific model that meets this need. Conventionally, the zenith hydrostatic delay, ZHD, is deployed for calculating DZD [*Tralli et al.*, 1992; *Rocken et al.*, 1995; *Bar-Sever and Kroger*, 1996; *Nam et al.*, 1996; *Duan et al.*, 1996]. According to *Davis et al.* [1985] and *Spilker* [1996], the ZHD is obtained by integrating the hydrostatic refractivity

$$N_h = 22.768\rho, \qquad (1)$$

where ρ is total tropospheric density, which includes the dry and wet densities. On the other hand, the DZD is generated through the integration of dry

[1] Now at Earth Orientation Department, U.S. Naval Observatory, Washington, D. C.

Paper number 1999RS900100.
0048-6604/00/1999RS900100$11.00

refractivity, which only includes the dry density. This difference, which may not be very significant sometimes, may introduce error to GPS meteorological applications as will be demonstrated in this study.

The ZHD can be calculated easily through surface meteorological observations making use of empirical models that have been developed for this need. The most popular ZHD models are the Saastamoinen (SAAS) [*Saastamoinen*, 1973] and Hopfield models [*Hopfield*, 1971]. Both models are in close agreement and do not produce significant differences in calculating ZHD.

In this study we first calibrate the ZHD model of SAAS using Hong Kong radiosonde data in situ such that it can be used in the computation of DZD for GPS-based meteorological applications. We then compare the predicted delays using the calibrated and uncalibrated models with the ones calculated from the radiosonde data. We also use the calibrated model in the GPS solutions to evaluate its performance.

2. ZHD Model and the Influence of Pressure Error

The ZHD is usually calculated using an empirical model that makes use of surface meteorological measurements. The model is assumed to be accurate enough to be considered without uncertainty [*Tralli et al.*, 1992; *Bar-Sever and Kroger*, 1996]. Several studies [*Bevis and Businger*, 1995; *Gendt and Beutler*, 1995; *Nam et al.*, 1996; *Dodson et al.*, 1996; *Duan et al.*, 1996] state that the existing empirical models are accurate to a few millimeters with the use of accurate surface pressure data. *Davis et al.* [1985] indicates that the uncertainty must be between 0.5 and 20 mm/1000 mbar. Nonetheless, no studies confirm their accuracies in detail. Moreover, despite the presence of numerous models for calculating the ZHD, there are very few studies about the use of ZHD for calculating the DZD in GPS applications, which is an adopted practice. Therefore, in this section we will first examine in detail how meteorological data affect the estimation of ZHD, and then compare the difference between the ZHD and the DZD derived from local radiosonde data.

The most popular ZHD model belongs to Saastamoinen [1973]. This model makes use of surface pressure measurement to estimate the hydrostatic delay along a vertical path through the total troposphere above a specific station.

The Saastamoinen model for ZHD is expressed as

$$d_S^z = 0.22768\frac{P}{F(\varphi, H)} \qquad (2)$$
$$F(\varphi, H) \equiv 1 - 0.0026\cos(2\varphi) - 0.00028H.$$

In the above expression, φ is the latitude of station in radians, H is the orthometric height or leveled height in kilometers, and P is the surface pressure measurement (total) in millibars at the station. The subscript S denotes that the ZHD is from the SAAS model. The unit of d_S^z is centimeters. The SAAS model is therefore dependent on the location of the site and the pressure but independent of the station temperature.

This model requires surface pressure measurements. Hence the accuracy of pressure directly affects the ZHD. In order to secure millimeter accuracy for the ZHD we need first to discuss and determine the admissible error in the surface pressure measurements.

If φ and H are known in (2) at a specific site, then the impact of the uncertainty in the pressure measurement P to the ZHD can be evaluated using the variance propagation laws on P, which gives

$$\sigma_{d_S^z} = \frac{0.2277}{F(\varphi, H)}\sigma_P. \qquad (3)$$

In the above relationship the coefficient of σ_P should be maximized for the largest impact on the ZHD. This condition is achieved only when φ is minimized and H is maximized in (3). Now, if we use φ=0° and H=9 km, which are quite extreme for the Earth, we obtain

$$\sigma_{d_S^z} = 0.2289\sigma_P. \qquad (4)$$

Here, the unit of ZHD is in centimeters and the pressure is in millibars. From (4), 0.4 mbar pressure measurement accuracy will guarantee that the ZHD precision will remain within 1 mm. This result is quite robust with respect to the current barometer standards. As a check, if we consider T=296.16 K, φ=22.15°, and H=0.114 km, representing the mean temperature and the location of a GPS station in Hong Kong, we obtain $\sigma_{d_S^z} = 0.2281\sigma_P$. This result indicates that if proper pressure measurements are made, we should expect that the influence of pressure error on the ZHD is < 1 mm in the SAAS model.

The ZHD is always larger than the DZD because the wet density is also included in the hydrostatic refractivity as shown in (1). Water vapor does not conform to the hydrostatic equation because water vapor is subject to myriad effects including condensation and exhibits large variations in concentration unlike the dry gases that are uniformly mixed [*Spilker*, 1996]. Thus there is no simple way to remove the water vapor from the ZHD relative to the surface water vapor pressure. To gain insight into the contribution of the water partial pressure in the zenith hydrostatic delay, we introduce the following independent reference standard for comparison.

3. Computing the DZD From Radiosonde Measurements and Its Uncertainty

The dry zenith delay d can be written as [*Dodson et al.*, 1996]

$$d = 10^{-6}\int N_d\,dh, \tag{5}$$

where N_d is the dry air refractivity and h is the height above the site.

A precise formula for the dry air refractivity by *Thayer* [1974] gives

$$N_d = 77.6\frac{P_d}{T}Z_d^{-1}$$

$$Z_d^{-1} = 1 + P_d[(57.90\times10^{-8})(1+\frac{0.52}{T}) - (9.4611\times10^{-4})\frac{t}{T^2}], \tag{6}$$

where P_d is the partial pressure of dry air in mbar, T is the temperature in Kelvin, and t is the temperature in degrees Celsius.

The dry partial pressure and temperature along the vertical path should be known to calculate the dry air refractivity along the vertical path, which can be provided by the radiosonde measurements. This information can then be used to convert the upper dry air refractivity into the dry delay in the vertical direction using the following approximation expression to (5):

$$d_R = 10^{-6}\sum_i (h_{i+1} - h_i)\frac{N_d^{i+1} + N_d^{i}}{2}, \tag{7}$$

where, the subscripts and superscripts i and $i+1$ denote the top and the bottom of each layer, respectively, for height and dry air refractivity. The DZD is function of dry partial pressure, temperature, and height. These observation errors of pressure, temperature, and height will propagate into the DZD via (6) and (7).

To analyze the impact of these observation errors, we differentiate (6). Neglecting Z_d^{-1} on the right-hand side, the differential relationship between N_d and P_d, T is

$$dN_d = \frac{77.6Z_d^{-1}}{T}dP_d - \frac{77.6P_dZ_d^{-1}}{T^2}dT. \tag{8}$$

The dry partial pressure is the difference of total pressure P and water pressure e so that

$$dP_d = dP - de. \tag{9}$$

Differentiating (7) and considering both (8) and (9) yields

$$dd_R = (0.5\times10^{-6})[\sum(N_d^{i+1} + N_d^{i})(dh_{i+1} - dh_i)$$

$$+ 77.6\sum(h_{i+1} - h_i)Z_d^{-1}(\frac{dP_i - de_i}{T_i} + \frac{dP_{i+1} - de_{i+1}}{T_{i+1}}$$

$$- \frac{P_d\,dT_i}{T_i^2} - \frac{P_{d_{i+1}}dT_{i+1}}{T_{i+1}^2}]. \tag{10}$$

Assuming that the measurements are uncorrelated and applying the variance propagation law to (10) gives

$$\sigma_{d_R} = \left[A\sigma_h^2 + B(\sigma_P^2 + \sigma_e^2) + C\sigma_T^2\right]^{1/2}, \tag{11}$$

where A, B, and C are defined by

$$A = (0.5\times10^{-12})\sum(N_d^{i+1} + N_d^{i})^2$$

$$B = (3.01088\times10^{-9})\sum(h_{i+1} - h_i)^2(\frac{1}{T_i^2} + \frac{1}{T_{i+1}^2})$$

$$C = (3.01088\times10^{-9})\sum(h_{i+1} - h_i)^2(\frac{P_{d_i}^2}{T_i^4} + \frac{P_{d_{i+1}}^2}{T_{i+1}^4}). \tag{12}$$

The empirical values for A, B, and C are given in Table 1. They are based on the 13-month radiosonde data collected in Hong Kong.

The empirical values for A, B, and C are given in Table 1. They are based on the 13-months Radiosonde data collected in Hong Kong.

Also, the height observation error σ_h is better than 1 m in GPS wind finding system employed in Hong Kong. Pressure and temperature measurement errors are σ_P=0.5 mbar, and σ_T=0.2 K (the RS80

Table 1. The Empirical Values for A, B, C, and the Corresponding σ_{d_R}

	Maximum	Minimum	Mean
A	1.38×10^{-4}	1.06×10^{-4}	1.24×10^{-4}
B	1.55×10^{-4}	0.77×10^{-4}	1.52×10^{-4}
C	3.13×10^{-4}	2.51×10^{-4}	2.95×10^{-4}
σ_{d_R}	2.3 mm	1.5 mm	2.3 mm

technical specifications are available from Vaisala Company: http://www.vaisala.com.). The water vapor pressure e can be calculated through temperature and relative humidity by an empirical formula [Massachusetts Institute of Technology (MIT), 1999]

$$e = RH \cdot [6.11\times10^{7.5t/(t+237.3)}] \qquad (13)$$

where RH is relative humidity and t is temperature in degrees Celsius. Similarly, it is easy to show that the accuracy σ_e of water vapor pressure should be better than 1.5 mbar considering that the maximum temperature is 40 °C in Hong Kong and the error of relative humidity is ~2% from radiosonde (from Vaisala Company "the RS80 technical specifications").

Substituting these values and those in Table 1 into (11) and expressing the resulting unit of millimeters, the corresponding σ_{d_t} is given in the last row of Table 1. These results show that the impact of the errors of the observed meteorological parameters as the DZD from the radiosonde data is ~2 mm.

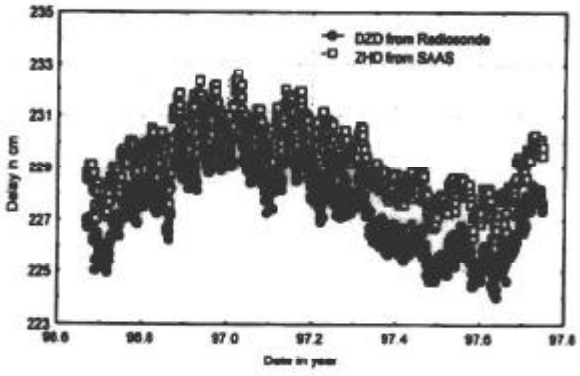

Figure 1. DZDs calculated from the radiosonde data and ZHDs from the SAAS model from September 1, 1996, to September 30, 1997.

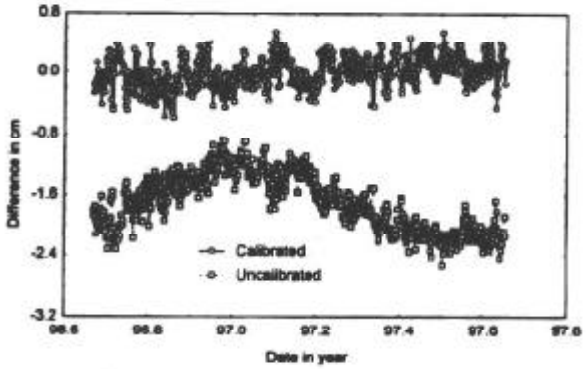

Figure 2. Differences between radiosonde and model before and after the calibration.

4. Difference Between DZD and ZHD

Because the radiosonde data are locally collected and accurate, we use them as a standard to compare the DZD to the ZHD computed from the empirical SAAS model. Figure 1 shows the ZHDs from the SAAS model and the DZDs calculated from the radiosonde data for the period of September 1, 1996, to September 30, 1997, that were collected twice daily by the Hong Kong Observatory in King's Park radiosonde station. The offset is clearly revealed in Figure 2, which is constructed using the differences between DZD computed from radiosonde data and ZHD from the SAAS models (we reserve one month of radiosonde data for model validation). Statistics for the differences between DZD from the radiosonde data and ZHD from the SAAS model show a 17 mm average offset with a standard deviation of 3.7 mm. The maximum and minimum differences are -8.7 mm and -25.4 mm, respectively. This systematic offset does not, however, fully explain all the variations that are present in the differences in Figure 2.

Figure 3 and Table 2 give the correlation between the differences and the pressure and temperature data used in calculating the model zenith delays. Theoretically, the difference between the DZD from the radiosonde and the ZHD from the SAAS model reveals the contribution of water vapor to ZHD. When the temperature is increasing, such as in summer, water vapor content of the troposphere is larger, and its contribution to the ZHD is larger. Consequently, the absolute difference between DZD and ZHD is larger while temperature is increasing. This is why the temperature is negatively correlated with the above differences. Water vapor pressure.

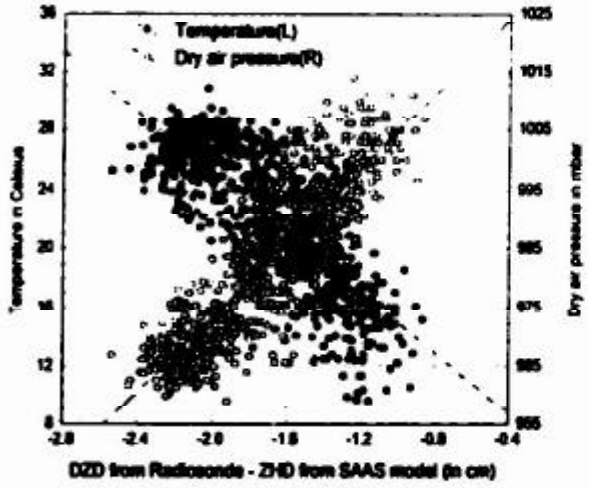

Figure 3. The correlation between the differences (DZD-ZHD) and the dry air pressure and temperature. Refer to Table 2 for the tabulated correlations.

which is calculated through temperature and relative humidity, becomes larger with the increasing temperature. Thus there is the negative 0.84 correlation between the DZD and ZHD differences and water vapor pressure.

The ZHD from the SAAS model is not as accurate as DZD from radiosonde data. The inaccuracy of ZHD may include other contributions besides the ones from water vapor. The uncertainty may be caused by the inaccuracy of model coefficient or the local variations that are not well represented by the existing model. This is also suggested by the positive 0.82 correlation between the DZD and ZHD differences and the total pressure in Table 2. These differences are positively correlated with total pressure but exhibit negative correlation with water vapor pressure. Actually, the sum of positive total pressure and negative pressure is just the value of the dry pressure. Thus the correlation between the dry pressure and the above differences implicitly includes the effects of both total pressure and water vapor pressure. This is why the correlation coefficient of dry pressure is larger than that of total pressure or water vapor pressure. For this reason we make use of the dry pressure in the following model calibration.

5. Model Calibration

As described by *Davis et al.* [1985] and *Spilker* [1996], the hydrostatic refractivity includes the tropospheric density, which is a function of the ratio of total pressure to the absolute temperature. We also adopt the similar expression, the ratio of dry pressure to the absolute temperature, in the following calibration model.

Considering our previous findings, we now postulate the following model

$$d_z - d_z^h = \delta + \mu \frac{P_d}{T} + \varepsilon. \tag{14}$$

Here, the difference in the left-hand side of (14) is the DZDs computed from radiosonde data and ZHDs from the SAAS model. Parameter δ represents the bias (constant part of the systematic differences) in centimeters in Figure 2, μ is the calibration scale factor in $cm\ K\ mbar^{-1}$ for the ratio of the dry air pressure to temperature, and ε denotes the random disturbances.

Using radiosonde data collected twice daily by the Hong Kong Observatory in King's Park radiosonde station, the model parameters δ and μ are estimated at 12.20 ± 0.26 cm and 3.153 ± 0.077 $cm\ K\ mbar^{-1}$, respectively, using the least squares technique. Estimated bias parameter is on the order of -12 cm. Its value is markedly large compared to the case when only the bias is estimated. The increase in magnitude in this case is due to the presence of the scale factor in the model and its correlation with the bias parameter in the estimation process.

An *F test* confirms that the estimated bias and scale parameters are statistically significant. The goodness-of-fit test has also been applied to test how well the model fits relative to the measurement errors. The testing results show that model fits are in agreement with the measurement errors. The adjusted differences when compared to the dry pressure and temperature (Figure 4) show that their correlations are markedly reduced as a result of the calibration.

In the above calibration model the uncertainty of dry pressure hardly affects the accuracy of the

Table 2. Correlation Coefficients Between the Radiosonde-Model Differences and Temperature and Pressure

Parameter	Radiosonde – SAAS Model
Total pressure P	0.82
Dry air pressure P_d	0.86
Wet vapor pressure	-0.84
Temperature (t in degrees Celsius)	-0.77
P_d/T ($T=t+273.16$)	0.83

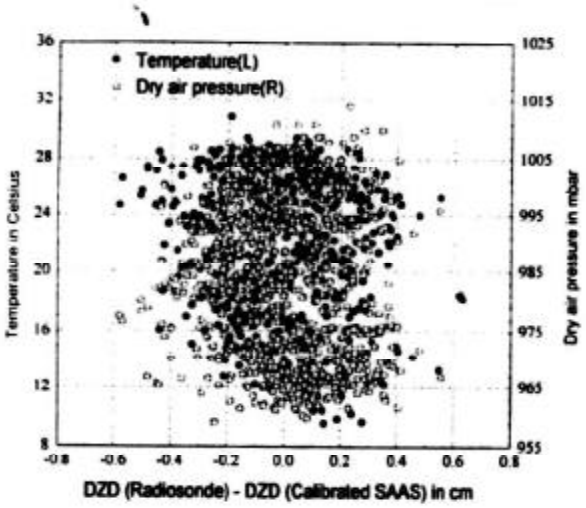

Figure 4. The correlations between the differences of DZDs (radiosonde –calibrated model) and the dry air pressure and temperature.

predicted DZD because of its small coefficient $3.15/T$. T is always larger than 270 K in Hong Kong, and the uncertainty of dry pressure is <2 mbar. Its impact on the predicted DZD is ~0.2 mm, so that we can neglect this effect.

6. Calibration Validation and Conclusion

To validate the calibration model given by (14), DZDs based on one-month radiosonde data that are not used in the estimation of calibration model parameters are compared to the zenith delays predicted by the calibrated models. Figure 5 shows the results of this comparison as well as those ZHDs

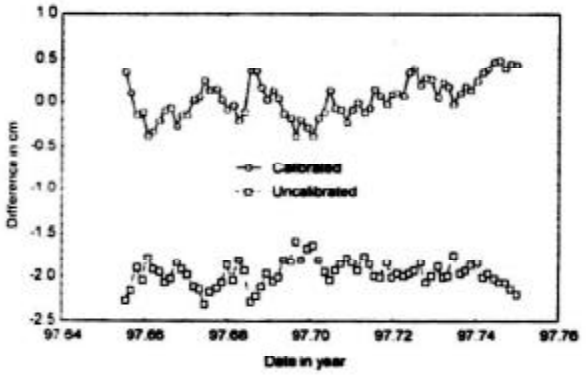

Figure 5. Differences between the predicted DZDs from the calibrated and uncalibrated models and DZDs calculated from the radiosonde data.

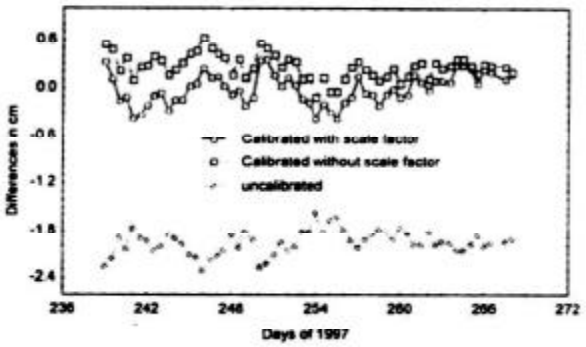

Figure 6. Differences between DZD from radiosonde and those from three methods for the period August 27 to September 27,1997.

obtained from the uncalibrated model. The major improvement is due to the removal of the bias between the empirical-model-based zenith hydrostatic delays and those from the radiosonde data.

We also considered the case where the calibration scale factor μ is neglected and only bias δ is considered in (14). The corresponding results appear in Figure 6. Obviously, the differences, without the scale factor in the model, still exhibit systematic differences when compared to the solution with the model including the scale factor. Hence the inclusion of the scale factor μ is needed in the calibration model. Observe that the distribution of the differences of radiosonde and predicted model DZDs concentrated about zero, which is a strong indicator of a well-calibrated model.

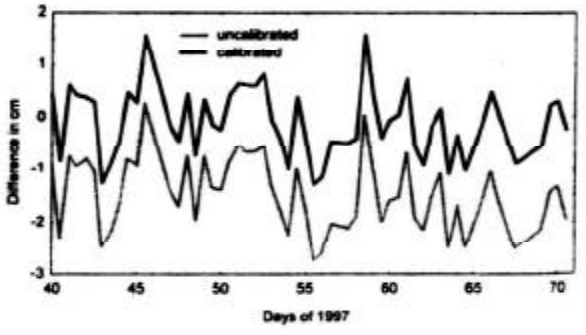

Figure 7. Differences of DZDs calculated from GPS data and the predicted DZDs from the calibrated and uncalibrated SAAS model (from February 09 to March 11 in 1997).

The statistics on the derivations between radiosonde and the predicted data from SAAS model, displayed in Figure 5, are as follows: uncalibrated model maximum, minimum, and mean are −1.58, -2.31, and −1.96, respectively; calibrated model values are 0.49, -0.37, and 0.05 respectively. If the models are not calibrated, they will, on the average, induce a systematic error ~2 cm in GPS measurements in Hong Kong, which is quite large for a multitude of GPS applications, as well as in computing wet zenith delays from GPS measurements.

In addition to the above approach we used GPS data to validate the calibration model. If the calibration were successful, we expect that the DZD which can be extracted from the total zenith delay estimated from GPS measurements would be in agreement with the DZDs predicted by the calibrated model using surface meteorological measurements.

To estimate the total zenith delays, we used one month's worth of GPS measurements collected with 2 min sampling interval in Hong Kong, together with five International GPS Service (IGS) stations in China. The data were analyzed using GAMIT software by forming daily session normal equations that include total zenith delay, in addition to the other relevant parameters (position, etc.), as a parameter to be estimated every 2 hours during the 24 hour period at each station. In data processing, the SAAS model is used to give the approximate zenith delay; the Niell mapping function model [*Niell*, 1996] is adopted, and the minimum elevation of 20° is used. The GPS receiver antenna and location are quite insensitive to the influence of multipath and interference. IGS antenna correction model has also been used to ensure the accurate estimation of tropospheric zenith delay [*Fang et al.*, 1998].

Using the radiosonde measurements that are collected in Hong Kong every 12 hour interval (0800 and 2000 LT) during the day, the wet zenith delay is calculated and subtracted from the estimated total zenith delay to obtain GPS-based DZD estimates in Hong Kong station.

Figure 7 shows the differences between these GPS-derived DZD estimates and the DZDs predicted by the calibrated model in Hong Kong station. The comparison of these results with uncalibrated DZD shows that the average differences can reach up to −1.45 cm over a month period, whereas the differences between the GPS-based DZDs and calibrated-model-predicted DZDs at the same epochs are distributed about zero with an average of 0.9 mm over the same period. Note also that the differences are noisy with standard deviation 6.6 mm over a month period as a result of limited precision in estimating total tropospheric delay from the GPS data and ~6.5 mm error of wet zenith delay from radiosonde [*Fang et al.*, 1998].

Acknowledgement. The Hong Kong Polytechnic University Grant Work Program, V366, supported this study. We are thankful to the Marine Department of Hong Kong for providing us the GPS data and to the Massachusetts Institute of Technology for the use of the GAMIT software. Comments and information provided by two careful reviewers are gratefully acknowledged.

References

Bar-Sever, Y. E., and P. M. Kroger, Strategies for GPS-based estimates of troposphere delay, paper presented at *the 9th International Technical Meeting of the Satellite Division of the Institute of Navigation*, Kansas City, Missouri, Sept. 17-20, 1996.

Bevis, M., and S. Businger, GPS meteorology and the International GPS Service, paper presented at *IGS 95 Workshop on Special Topics and New Directions*, Int. GPS Serv., Potsdam, Germany, May 15-18, 1995.

Davis, J. L., T. A. Herring, I. I. Shapiro, A. E. E. Rogers, and G. Elgered, Geodesy by radio interferometry: Effects of atmospheric modeling errors on estimates of baseline length, *Radio Sci.*, *20*, 6, 1593-1607, 1985.

Dodson, A. H., P. J. Shardlow, L. C. M. Hubbard, G. Elgered, and P. O. J. Jarlemark, Wet tropospheric effects on precise relative GPS height determination, *J. Geod.*, *70*, 188-202, 1996.

Duan, J., et al., GPS meteorology: Direct estimation of the absolute value of precipitable water, *J. Appl. Meteorol.*, *35*, 830-838, 1996.

Fang, P., M. Bevis, Y. Bock, S. Gutman, and D. Wolfe, GPS meteorology: Reducing systematic errors in geodetic estimates for zenith delay, *Geophy. Res. Lett.*, *25*, 19, 3583-3586, 1998.

Gendt G., and G. Beutler, Consistency in the troposphere estimations using the IGS network, paper presented at *IGS 95 Workshop on Special Topics and New Directions*, Int. GPS Serv., Potsdam, Germany, May 15-18, 1995.

Hopfield, H. S., Tropospheric effect on electromagnetically measured range: Prediction from surface weather data, *Radio Sci.*, *6*, 3, 357-367, 1971.

Massachusetts Institute of Technology (MIT), GAMIT software, 1999.

Nam, Y. S., D. Kuang, and B. E. Schutz, Comparison of GPS estimates of wet tropospheric delays with WVR measurements, paper presented at *the 9th International*

Technical Meeting of the Satellite Division of the Institute of Navigation. Kansas City, Missouri, Sept. 17-20, 1996.

Niell, A. E., Global mapping functions for the atmosphere delay at radio wavelengths, *J. Geophy. Res.*, *101*, 3227-3246, 1996.

Rocken C., F. S. Solheim, R. H. Ware, M. Exner, D. Martin, and M. Rothacher, Application of IGS data to GPS sensing of the atmosphere for weather and climate research, paper presented at *IGS 95 Workshop on Special Topics and New Directions*, Int. GPS Serv., Potsdam, Germany, May 15-18, 1995.

Saastamoinen, J., Contributions to the theory of atmospheric refraction, part II, Refraction corrections in satellite geodesy, *Bull. Geod.*, *107*, 13-34, 1973.

Spilker, J. J., Jr., Tropospheric effects on GPS, *Global Positioning System: Theory and Applications*, edited by B. W. Parkinson, chap. 13, pp. 517-546, American Institute of Aeronautics and Astronautics Inc., Washington, DC, 1996.

Thayer, G. D., An improved equation for the radio refractive of air. *Radio Sci.*, *9*, 10, 803-807, 1974.

Tralli, D. M., S. M. Lichten, and T. A. Herring, Comparison of Kalman filter estimates of zenith atmospheric path delays using the Global Positioning System and very long baseline interferometry, *Radio Sci.*, *27*, 999-1007, 1992.

H. Baki. Iz, Earth Orientation Department, U.S. Naval Observatory, Washington, D .C. 20392-5420.

Y. Chen and Y. Liu, Department of Land Surveying and Geo-Informatics, Hong Kong Polytechnic University, Hung Hom, Kowloon, Hong Kong. (lsyqchen@polyu.edu.hk, 96980619r@polyu.edu.hk).

(Received February 8, 1999; revised September 7, 1999; accepted September 13, 1999.)